Structural Engineering and Mechanics, Vol. 39, No. 2 (2011) 267-285
DOI: http://dx.doi.org/10.12989/sem.2011.39.2.267

Prediction of moments in composite frames considering cracking and time effects using neural network models

Umesh Pendharkar[1a], Sandeep Chaudhary[2b] and A.K. Nagpal*[3]

[1]*Civil Engineering, Ujjain Engineering College, Ujjain, India*
[2]*Structural Engineering, Malaviya National Institute of Technology, Jaipur, India*
[3]*Civil Engineering, Indian Institute of Technology Delhi, New Delhi, India*

(Received June 3, 2010, Accepted April 6, 2011)

Abstract. There can be a significant amount of moment redistribution in composite frames consisting of steel columns and composite beams, due to cracking, creep and shrinkage of concrete. Considerable amount of computational effort is required for taking into account these effects for large composite frames. A methodology has been presented in this paper for taking into account these effects. In the methodology that has been demonstrated for moderately high frames, neural network models are developed for rapid prediction of the inelastic moments (typically for 20 years, considering instantaneous cracking, and time effects, i.e., creep and shrinkage, in concrete) at a joint in a frame from the elastic moments (neglecting instantaneous cracking and time effects). The proposed models predict the inelastic moment ratios (ratio of elastic moment to inelastic moment) using eleven input parameters for interior joints and seven input parameters for exterior joints. The training and testing data sets are generated using a hybrid procedure developed by the authors. The neural network models have been validated for frames of different number of spans and storeys. The models drastically reduce the computational effort and predict the inelastic moments, with reasonable accuracy for practical purposes, from the elastic moments, that can be obtained from any of the readily available software.

Keywords: composite frames; cracking; creep; shrinkage; neural networks

1. Introduction

There has been an extensive use of concrete slab in steel framed buildings. The monolithic action of concrete slab and steel beams leads to the composite beam action (Fig. 1, Pendharkar *et al.* 2007).

In frames of moderate height, in end regions of composite beams of composite frames hogging moments occur whereas in the middle region sagging moment occurs. There is instantaneous cracking of concrete in end regions when the hogging moments are higher than cracking moment, M^{cr} (moment causing cracking in extreme fibre of concrete). The instantaneous cracking at a joint results in lower moments at the joint and higher span moments and higher moments at the adjacent

*Corresponding author, Professor, E-mail: aknagpal@civil.iitd.ernet.in
[a]Professor
[b]Associate Professor

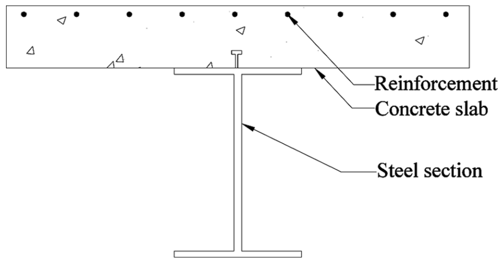

Fig. 1 Cross-section of composite beam (Pendharkar *et al.* 2007)

joints. The change in moments at the adjacent joints is however much smaller than at the joint where cracking takes place. This effect progresses to joints farther away from the adjacent joints also. This is one cause for redistribution of moments. The other cause for the redistribution is the occurrence of time dependent effects of creep and shrinkage in concrete. Creep and shrinkage result in increase in elastic moments at joints (Ghali *et al.* 2002, Pendharkar 2007, Chaudhary *et al.* 2007a). Further it has been shown that increase in moments at joints is primarily due to shrinkage, the contribution of creep being much smaller (Ghali *et al.* 2002, Pendharkar 2007, Chaudhary *et al.* 2007a). However, cracking in concrete results in lesser increase in moments as the portion of the concrete undergoing creep and shrinkage reduces (Gilbert and Bradford 1995, Bradford *et al.* 2002, Kwak and Seo 2000).

Methods are available in the literature for instantaneous and time-dependent analysis of the beams and frames, which take into account these moment redistributions. For instantaneous analysis, conventionally either an incremental or an iterative approach (Ghali *et al.* 2002) is used which requires subdivisions and thereby numerical integration. The computational effort required in numerical integration may be considerable in case of large structures. For time-dependent analysis of composite structures, a large number of methods are available in the literature and they may be categorized in two types. Type 1 methods are numerical in nature and require large computational effort (Cruz *et al.* 1998, Kwak and Seo 2000, Mari 2000, Fragiacomo *et al.* 2004) and Type 2 methods are analytical in nature and are computationally efficient but these methods do not take into account all the aspects (Gilbert and Bradford 1995, Amadio and Fragiacomo 1997, Bradford *et al.* 2002). Recently, a hybrid analytical-numerical procedure has been developed (Chaudhary *et al.* 2007b) to take into account the non-linear effects of concrete cracking and time-dependent effects of creep and shrinkage in composite frames. The procedure is efficient but the computational effort may again become considerable for large composite building frames. This effort may be many times more than that required for the elastic analysis (neglecting cracking and time effects in concrete). The use of neural network models may be made to drastically reduce the computational effort in such cases.

Neural networks have been widely used for the prediction of various structural quantities (Mo *et al.* 2002, Jeng and Mo 2004, Akbas 2006, Giri and Upadhyay 2006, Arslan *et al.* 2007, Cheng *et al.* 2007, Chandak *et al.* 2008, Pendharkar *et al.* 2010), structural damage diagnosis and detections (Cho *et al.* 2004, Lee *et al.* 2005, Yeung and Smith 2005, Jiang *et al.* 2006, Bakhary *et al.* 2007), active response control of offshore structures (Kim *et al.* 2009a, Chang *et al.* 2009) and static model identification of an FRP deck (Kim *et al.* 2009b) etc. Neural networks thus have been a powerful tool in solution of various structural engineering problems. Recently, neural networks have been developed for evaluation of redistribution of moments in the continuous composite beams due to cracking (Chaudhary *et al.* 2007c) as well as due to cracking and time-dependent effects (Pendharkar *et al.* 2007).

A methodology has been presented in this paper for rapid prediction of moments in large composite frames taking into account cracking, creep and shrinkage. The methodology has been demonstrated for moderately high composite frames. In the methodology, neural networks are developed to estimate inelastic moments, M^i (considering cracking and time effects in concrete) from elastic moments, M^e (neglecting cracking and time effects in concrete). M^e can be obtained from any of the readily available softwares and requires little computational effort. Thus there is also a drastic reduction in computational effort required in evaluation of M^i. Multilayered feed-forward networks have been developed using sigmoid function as an activation function and the back propagation-learning algorithm for training. Training and testing patterns for developing the neural networks are created using the hybrid procedure (Chaudhary *et al.* 2007b) developed by the authors. The neural network models have been validated for frames of different number of spans and storeys. The errors are shown to be small for practical purposes. A sensitivity analysis is also carried out to obtain the effect of each parameter and thereby to identify the significant parameters.

2. Structural parameters

As stated earlier in section 1, instantaneous cracking in composite beams of frames occurs in the end portions (where hogging moments occur) when tensile stresses are higher than the tensile strength of concrete. This instantaneous cracking may further progress due to time effects. The elastic bending moment M^e at an instantaneous stage gets redistributed owing to cracking and there is a further redistribution owing to time effects of creep and shrinkage leading to M^i at a final stage (typically 20 years).

It has been shown in earlier studies (Chaudhary *et al.* 2007c, Pendharkar *et al.* 2007) for a continuous composite beam, that in order to establish redistribution of moment at a support j with sufficient accuracy, cracking at the support and adjacent supports (support $j-1$ and support $j+1$)

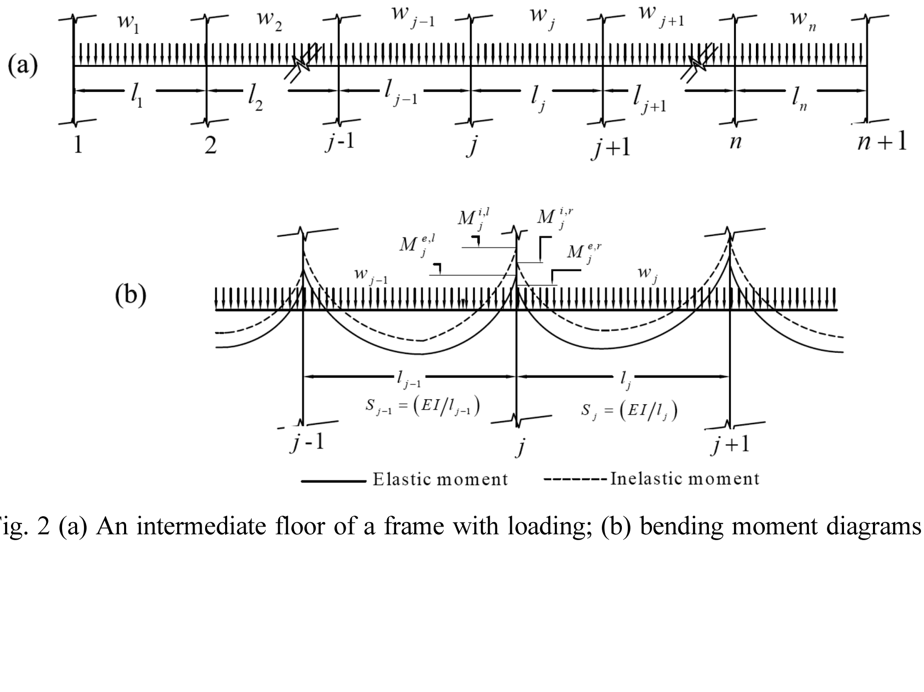

Fig. 2 (a) An intermediate floor of a frame with loading; (b) bending moment diagrams only needs to be considered.

Consider now, an intermediate floor of a frame with the loading (Fig. 2(a)). The nature of elastic moment diagram and inelastic moment diagram at a joint j of an intermediate floor of a frame is shown in the Fig. 2(b).

The outputs for the neural network model for an internal joint, j, are considered as $M_j^{e,l}/M_j^{i,l}$ (inelastic moment ratio to the left of joint j) and $M_j^{e,r}/M_j^{i,r}$ (inelastic moment ratio to the right of joint j).

Since cracking and creep and shrinkage effects, in the type of frames being considered, are confined to beams only, it may be postulated based on the studies on the composite beams (Chaudhary *et al.* 2007c), that in order to establish redistribution of moment at a joint, cracking at the joint and adjacent joints only needs to be considered. Keeping this in view, the following input parameters for an internal joint j of a frame are identified.

1. Stiffness ratio of adjacent spans, S_{j-1}/S_j.
2. Load ratio of the adjacent spans, w_{j-1}/w_j.
3. Cracking moment ratio on the left side of the joint, $R_j^l = (M^{cr}/M_j^{e,l})$
4. Cracking moment ratio on the right side of the joint, $R_j^r = (M^{cr}/M_j^{e,r})$.
5. Cracking moment ratio on left side of the left adjacent joint, $R_{j-1}^l = (M^{cr}/M_{j-1}^{e,l})$.
6. Cracking moment ratio on right side of left adjacent support, $R_{j-1}^r = (M^{cr}/M_{j-1}^{e,r})$.
7. Cracking moment ratio on left side of right adjacent support, $R_{j+1}^l = (M^{cr}/M_{j+1}^{e,l})$.
8. Cracking moment ratio on right side of right adjacent support, $R_{j+1}^r = (M^{cr}/M_{j+1}^{e,r})$.
9. Composite inertia ratio, I^{cr}/I^{un}, where I^{cr} = transformed moment of inertia of steel section.

Additionally, in order to take into account the effect of creep and shrinkage, the following parameters are also identified (Pendharkar 2007).

10. Grade of concrete, Gr.
11. Age of loading, t_0.

These input parameters are schematically shown in Fig. 3. The practical ranges for the different structural parameters are considered as: $S_{j-1}/S_j = 0.25 - 4.0$; $w_{j-1}/w_j = 0.25 - 4.0$; $R_{j-1}^l = 0.25 - 4.0$; $R_{j-1}^r = 0.25 - 4.0$; $R_j^l = 0.25 - 4.0$; $R_j^r = 0.25 - 4.0$; $R_{j+1}^l = 0.25 - 4.0$; $R_{j+1}^r = 0.25 - 4.0$; $I^{cr}/I^{un} = 0.38 - 0.54$; $Gr = 20\ \text{N/mm}^2 - 40\ \text{N/mm}^2$; $t_0 = 7$ days $-$ 21 days.

It may be noted that the ratio of beam stiffness to column stiffness is not taken as input parameter

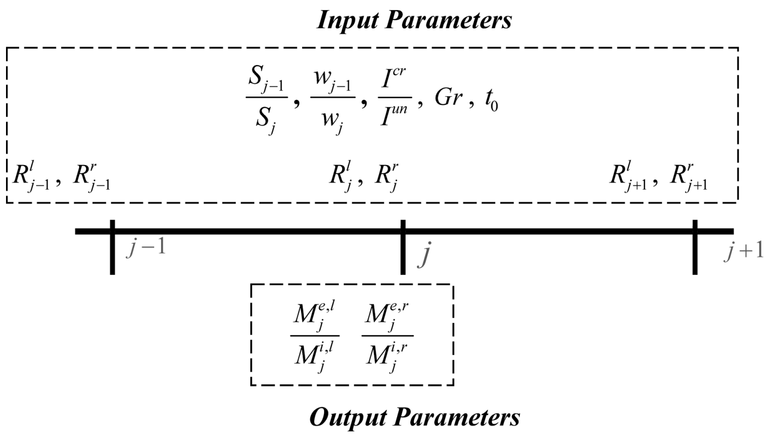

Fig. 3 Schematic representation of input and output parameters

since in the output parameters $M_j^{e,l}/M_j^{i,l}$ and $M_j^{e,r}/M_j^{i,r}$ both M^e and M^i may be assumed to be affected approximately to the same degree by variation in ratio of beam to column stiffness.

All the neural networks would be trained for a particular value of relative humidity, *RH*. This value is designated here as RH_1 and is taken as equal to 85%. The output parameter for other values of relative humidity, RH_2, can then be estimated as explained below.

It has been established that the time-dependent change in bending moment is primarily due to shrinkage and the effect of creep is negligible (Chaudhary *et al.* 2007a, Pendharkar 2007). Shrinkage strain depends on, besides relative humidity, *RH*, several factors. It can be expressed as (CEB-FIP MC 90 1993)

$$\varepsilon_{sh} = (K)\left[1-\left(\frac{RH}{100}\right)^3\right] \quad \text{for} \quad 40\% \le RH \le 99\% \tag{1}$$

where, *K* represents the effect of all factors other than *RH*.

In absence of cracking, the time-dependent change in bending moments, $M_j^{i,l}-M_j^{e,l}$ or $M_j^{i,r}-M_j^{e,r}$ result from shrinkage and their variation with relative humidity can be expressed as

$$\Delta M_j^l = M_j^{i,l}-M_j^{e,l} = C^l[1-0.01(RH)^3] \tag{2}$$

$$\Delta M_j^r = M_j^{i,r}-M_j^{e,r} = C^r[1-0.01(RH)^3] \tag{3}$$

where, C^l and C^r are constants of proportionality that depend on structural and material properties.

Eqs. (2) and (3) though strictly valid in absence of cracking may however be assumed to hold good when cracking is present.

The ratio of changes in ΔM_j^l and ΔM_j^r at two different values of *RH*, viz. RH_1 and RH_2 can be expressed as

$$\frac{\Delta M_{j,1}^l}{\Delta M_{j,2}^l} = \frac{M_{j,1}^{i,l}-M_j^{e,l}}{M_{j,2}^{i,l}-M_j^{e,l}} = \frac{[1-0.01(RH_1)^3]}{[1-0.01(RH_2)^3]} \tag{4}$$

$$\frac{\Delta M_{j,1}^r}{\Delta M_{j,2}^r} = \frac{M_{j,1}^{i,r}-M_j^{e,r}}{M_{j,2}^{i,r}-M_j^{e,r}} = \frac{[1-0.01(RH_1)^3]}{[1-0.01(RH_2)^3]} \tag{5}$$

where, $M_{j,1}^{i,l}$ and $M_{j,2}^{i,l}$ are values of $M_j^{i,l}$ at $RH = RH_1$ and RH_2. Similarly, $M_{j,1}^{i,r}$ and $M_{j,2}^{i,r}$ are values of $M_j^{i,r}$ at $RH = RH_1$ and RH_2.

From Eqs. (4) and (5), $M_{j,2}^{i,l}$ and $M_{j,2}^{i,r}$ can be expressed as

$$M_{j,2}^{i,l} = M_j^{e,l}+(M_{j,1}^{i,l}-M_j^{e,l}) = \frac{[1-0.01(RH_2)^3]}{[1-0.01(RH_1)^3]} \tag{6}$$

$$M_{j,2}^{i,r} = M_j^{e,r}+(M_{j,1}^{i,r}-M_j^{e,r}) = \frac{[1-0.01(RH_2)^3]}{[1-0.01(RH_1)^3]} \tag{7}$$

As stated earlier, training will be carried out for RH_1 (= 85%) from which $M_{j,2}^{i,l}$ and $M_{j,2}^{i,r}$, for any other value of relative humidity, RH_2 can be estimated using Eqs. (6) and (7).

3. Configuration of neural network models

The neural network model chosen in the present study is a multilayered feed-forward network with neurons in all the layers fully connected in feed-forward manner (Fig. 4). Sigmoid function is used as an activation function and the back propagation-learning algorithm is used for training.

First, consider the neural network model for an internal joint. As stated earlier in section 2, the neural network model consists of eleven input parameters and two output parameters. The eleven input parameters are: $S_{j-1}/S_j, w_{j-1}/w_j, R^l_{j-1}, R^r_{j-1}, R^l_j, R^r_j, R^l_{j+1}, R^r_{j+1}, I^{cr}/I^{un}, Gr$ and t_0. The two output parameters are: $M^{e,l}_j/M^{i,l}_j$ and $M^{e,r}_j/M^{i,r}_j$.

Next, consider the neural network model for an external joint. The input parameters S_{j-1}/S_j, $w_{j-1}/w_j, R^l_{j-1}$ and R^r_{j-1} are absent for left external joint (j = 1) and a particular value, say equal to 10.0, is assumed for $M^{cr}/M^{e,l}_j$. On encountering this value, the neural network would identify this joint as left external joint (joint 1). Similarly, the input parameters S_{j-1}/S_j, $w_{j-1}/w_j, R^l_{j+1}$ and R^r_{j+1} are absent for right external joint ($j = n+1$). Again, a particular value say equal to 10.0 is assumed for $M^{cr}/M^{e,r}_j$. Thus for the two external joints, the input consists of seven parameters each. The input parameters for left external joint (joint 1) are: $R^l_1, R^r_1, R^l_2, R^r_2, I^{cr}/I^{un}, Gr$ and t_0, whereas, the parameters for right external joint (joint $n+1$) are $R^l_n, R^r_n, R^l_{n+1}, R^r_{n+1}, I^{cr}/I^{un}, Gr$ and t_0. The output parameters are $M^{e,r}_1/M^{i,r}_1$ and $M^{e,l}_{n+1}/M^{i,l}_{n+1}$ for left external joint and right external joint respectively.

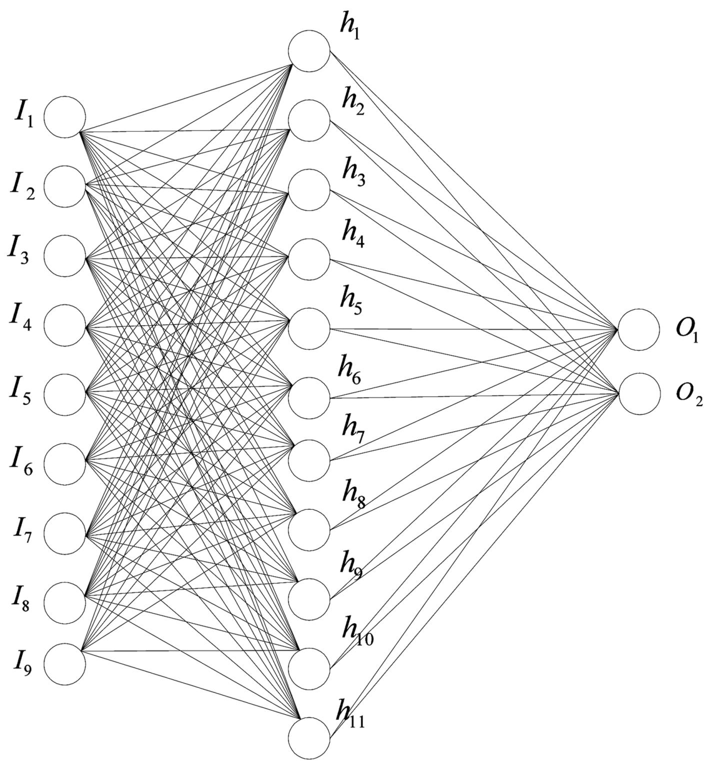

Fig. 4 A typical neural network model

4. Training of neural network

A beam of a frame may be considered as a continuous beam in which columns of upper and lower storey provide rotational restraints (Fig. 5(a)) at the joints. This in turn may be represented by an equivalent single storey frame (Fig. 5(b)) in which the columns provide the rotational restraints. Therefore a single storey frame has been used to generate training data sets (combination of different values of input parameters and the corresponding values of output parameters).

All the data sets are generated for a single storey seven bay frame, henceforth designated as data generation frame. It is postulated that neural network models based on these training data sets are applicable for predicting $M_j^{e,l}/M_j^{i,l}$ and $M_j^{e,r}/M_j^{i,r}$ for frames of any number of spans and storeys.

Two neural network models, one each for external joints and internal joints and designated as Net-external and Net-internal are trained. Input data sets have been chosen to cover the entire practical range of parameters and sufficiently large number of values of each of the parameters. A training data set, typically for interior joint, consists of eleven input parameters and two output parameters. In order to have specified values of eleven input parameters of a data set, an iterative procedure needs to be followed. The variables, for the data generation frame, in this iterative procedure are seven span lengths, seven corresponding loadings on the spans, cross-sectional properties, and grade of concrete and age of loading. The values of the variables are adjusted in such a manner that the specified values of eleven input parameters are achieved. The inelastic moments, $M_j^{i,l}$ and $M_j^{i,r}$ required in the output parameters are obtained by using the hybrid procedure (Chaudhary *et al.* 2007b) briefly described below.

Hybrid Procedure: In this procedure, a span length cracked beam element consisting of an uncracked zone in the middle and cracked zones at the ends (Fig. 6(a), Chaudhary *et al.* 2007b, Pendharkar *et al.* 2007) has been used. The analysis is carried out in two parts. In the first part, an instantaneous analysis is carried out using an iterative method. In the second part, a time-dependent analysis is carried out by dividing the time into a number of time intervals to take into account the progressive nature of cracking of concrete (Fig. 6(b), Chaudhary *et al.* 2007b, Pendharkar *et al.* 2007). As shown in the figure, crack lengths are assumed to be constant in a time-interval and

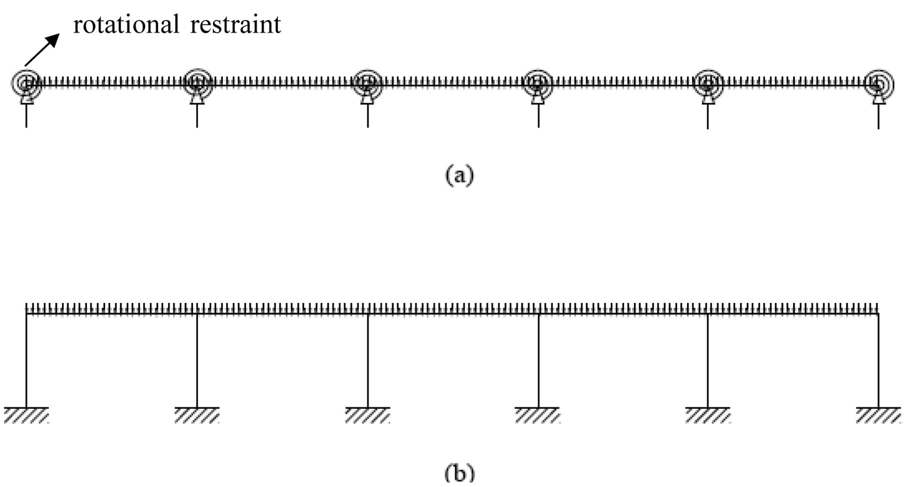

Fig. 5 (a) Continuous composite beam with rotational restraints, (b) an equivalent single storey frame

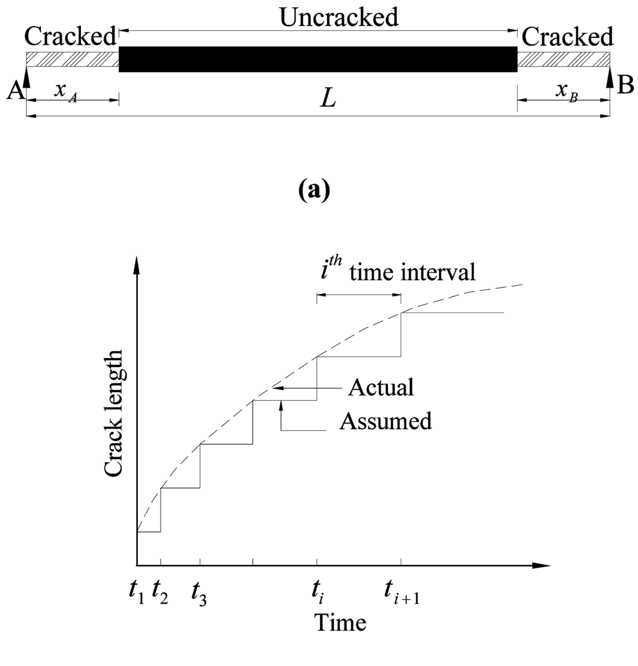

(b)

Fig. 6 (a) Span length cracked beam element, (b) progressive nature of cracking (Chaudhary *et al*. 2007b, Pendharkar *et al.* 2007)

Table 1 Normalization factors

Network	Joint	Normalisation factor												
		Input											Output	
		$\frac{S_{j-1}}{S_j}$	$\frac{w_{j-1}}{w_j}$	R^l_{j-1}	R^r_{j-1}	R^l_j	R^r_j	R^l_{j+1}	R^r_{j+1}	$\frac{I^{cr}}{I^{un}}$	Gr (N/mm^2)	t_0 (days)		
Net-external	Left External	-	-	-	-	10.05	4.05	4.05	4.05	1	41	22	-	20
	Right External	-	-	4.05	4.05	4.05	10.05	-	-	1	41	22	20	-
Net-internal	Internal	4.05	4.05	10.05	4.05	4.05	4.05	4.05	10.05	1	41	22	3.0	3.0

revised at the end of each time interval. The age-adjusted effective modulus method, AAEMM (Bazant 1972) is used for predicting the creep and shrinkage effects whereas CEB-FIP MC 90 (1993) is used for predicting the short term as well as time-dependent properties of the concrete. The hybrid procedure has been validated by Chaudhary *et al.* (2007b) with the experimental, analytical and Finite Element results.

The ratios of elastic and inelastic moments obtained from the hybrid procedure form the output parameters. As stated earlier, each combination of different values of input parameters and the corresponding values of output parameters forms a data set. For the networks Net-external and Net-

Table 2 Configuration of networks, mean square errors, square of coefficient of correlation and number of epochs

Network	Configuration	MSE		R_c^2		Epochs
		Training	Testing	Training	Testing	
NETFM1	7-15-1	0.00089	0.00159	0.968	0.957	55000
NETFM2	11-15-2	0.00029	0.00212	0.953	0.914	55000

internal, 3050 and 55,000 data sets, in the practical ranges of the parameters, are generated respectively.

To bring all the input parameters and output parameters in the range 0.0 to 1.0, the inputs as well as the output parameters are divided by the normalization factors given in Table 1.

The training is carried out using the Stuttgart Neural Network Simulator (SNNS 1998). For training, several trials with different numbers of neurons on the hidden layer are carried out. Two third of data sets are used for training as training patterns whereas one third of data sets are used for testing. The configurations of the two optimum networks (number of input parameters-number of neurons in hidden layer-number of output parameters) along with mean square error MSE, square of coefficient of correlation R_c^2, and number of epochs are given in Table 2. The value of R_c^2 for all the networks is greater than 0.9 for both training and testing data sets. The networks therefore have a good generalization capability.

5. Validation of neural networks

Trained neural networks are validated for different frames with a wide variation of input parameters. These parameters are in different permutations than that used in the training. The

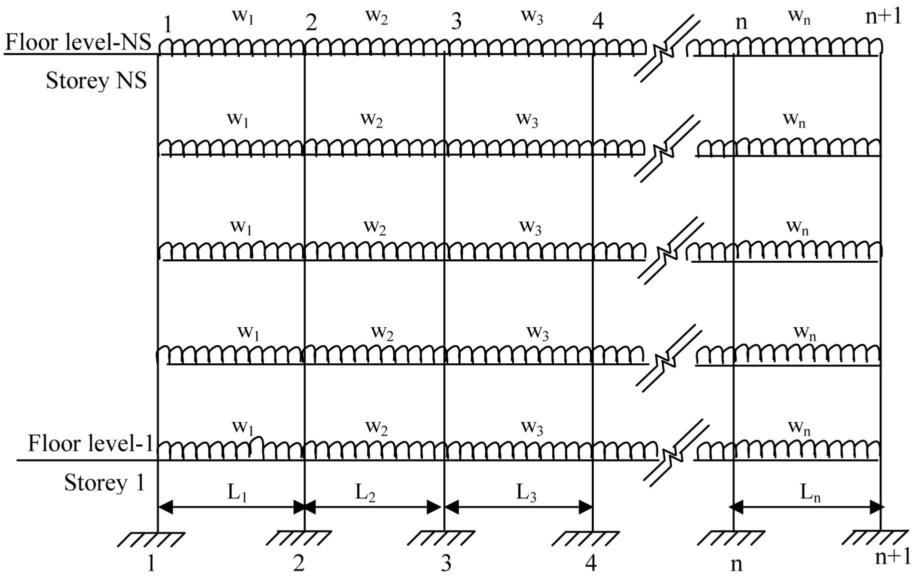

Fig. 7 Schematic representation of example frames

Table 3 Details of example frames

Frame		Beams: Spans 1	2	3	4	5	6	7	8	Concrete Slab Gr (N/mm^2)	Concrete Slab Size (mm)	Steel Section	Column Section: Storey 1	2	3	4	5	t_0 (days)	RH_2 (%)
EF 1	Length (m)	8.0	5.0	6.0	5.0	2.0	4.0	7.0	9.0	35	1000 ×75	356× 171 UB 67	203× 133 UB 30	-	-	-	-	19	78
	Load (kN/m)	19.0	24.0	27.0	24.0	14.0	16.0	18.0	20.0										
EF 2	Length (m)	4.0	3.0	4.0	6.0	-	-	-	-	30	900 ×90	356×171 UB 67	356× 171 UB 67	356× 171 UB 51	305× 165 UB 40	203× 133 UB 30	305× 102 UB 25	10	70
	Load (kN/m)	30.0	35.0	25.0	20.0	-	-	-	-										

Table 4 Input parameters for example frame EF1

Joint	Floor Lvel.	Joint No.	$\frac{S_{j-1}}{S_j}$	$\frac{w_{j-1}}{w_j}$	R^l_{j-1}	R^r_{j-1}	R^l_j	R^r_j	R^l_{j+1}	R^r_{j+1}	$\frac{I^{cr}}{I^{un}}$	Gr (N/mm^2)	t_0 (days)
External	1st	1	-	-	-	-	0.995*	0.668	0.121	0.053	0.433	0.854	0.864
		9	-	-	0.145	0.087	0.482	0.995*	-	-	0.433	0.854	0.864
Internal	1st	2	0.154	0.195	0.995*	0.668	0.121	0.131	0.236	0.088	0.433	0.854	0.864
		3	0.296	0.219	0.049	0.131	0.236	0.218	0.169	0.070	0.433	0.854	0.864
		4	0.206	0.278	0.095	0.218	0.169	0.174	0.468	0.201	0.433	0.854	0.864
		5	0.099	0.423	0.068	0.174	0.468	0.498	0.947	0.357	0.433	0.854	0.864
		6	0.494	0.216	0.189	0.498	0.947	0.887	0.380	0.145	0.433	0.854	0.864
		7	0.432	0.219	0.382	0.887	0.380	0.360	0.094	0.035	0.433	0.854	0.864
		8	0.317	0.222	0.153	0.360	0.094	0.087	0.482	0.995*	0.433	0.854	0.864

* = Boundary Condition.

example frames are shown schematically in Fig. 7.

Two composite frames of single storey (frame EF1) and five storey (frame EF2) are considered for validation (Fig. 7, n = 4 and 8 for EF1 and EF2 respectively). The details of example frames are given in Table 3. The slabs of composite beams of the frames have a reinforcement of area 508 mm^2 placed at a distance of 15 mm from the top fiber.

Results are reported for floor level 1 for frame EF1 and floor levels 1, 3 and 5 for frame EF2. The network Net-external is used for external joints (joints 1 and 9 for frame EF1 and joints 1 and 5 for frame EF2) whereas network Net-internal is used for internal joints (joints 2 to 8 for frame EF1 and joints 2 to 4 for frame EF2). Tables 4 and 5 show the values of the input parameters for the external and internal joints of the example frames EF1 and EF2 respectively. As stated earlier, these parameters are in different permutations than those used in training.

The values of inelastic moments $M_j^{i,l}$ and $M_j^{i,r}$ obtained from neural networks are compared with those obtained from the hybrid procedure and the errors found in prediction of inelastic moments, for example frames EF1 and EF2, are shown in Tables 6 and 7 respectively. The values of elastic

Table 5 Input parameters for example frame EF2

Joint	Floor Lvel.	Joint No.	$\frac{S_{j-1}}{S_j}$	$\frac{w_{j-1}}{w_j}$	R^l_{j-1}	R^r_{j-1}	R^l_j	R^r_j	R^l_{j+1}	R^r_{j+1}	$\frac{I^{cr}}{I^{un}}$	Gr (N/mm^2)	t_0 (days)
External	1st	1	-	-	-	-	0.995*	0.327	0.319	0.148	0.476	0.732	0.455
		5	-	-	0.101	0.184	0.228	0.995	-	-	0.476	0.732	0.455
	3rd	1	-	-	-	-	0.995*	0.372	0.430	0.179	0.476	0.732	0.455
		5	-	-	0.097	0.199	0.276	0.995*	-	-	0.476	0.732	0.455
	5th	1	-	-	-	-	0.995*	0.588	0.498	0.201	0.476	0.732	0.455
		5	-	-	0.091	0.203	0.439	0.995*	-	-	0.476	0.732	0.455
Internal	1st	2	0.185	0.212	0.995	0.327	0.319	0.367	0.387	0.144	0.476	0.732	0.455
		3	0.329	0.346	0.129	0.367	0.387	0.357	0.250	0.074	0.476	0.732	0.455
		4	0.370	0.309	0.156	0.357	0.250	0.184	0.228	0.995	0.476	0.732	0.455
	3rd	2	0.185	0.212	0.995	0.372	0.430	0.445	0.316	0.124	0.476	0.732	0.455
		3	0.329	0.346	0.173	0.445	0.316	0.307	0.241	0.080	0.476	0.732	0.455
		4	0.370	0.309	0.127	0.307	0.241	0.199	0.276	0.995	0.476	0.732	0.455
	5th	2	0.185	0.212	0.995	0.588	0.498	0.499	0.291	0.116	0.476	0.732	0.455
		3	0.329	0.346	0.201	0.499	0.291	0.287	0.227	0.082	0.476	0.732	0.455
		4	0.370	0.309	0.117	0.287	0.227	0.203	0.439	0.995	0.476	0.732	0.455

* = Boundary Condition

Table 6 Comparison of inelastic moments obtained from the neural networks and the hybrid procedure for frame EF1 (RH=78%)

Floor Level	Joint	Elastic moment (kN·m)		Inelastic moment (kN·m)				% error	
				Hybrid Procedure		Neural Network			
	j	$M_j^{e,l}$	$M_j^{e,r}$	$M_j^{i,l}$	$M_j^{i,r}$	$M_j^{i,l}$	$M_j^{i,r}$	$M_j^{i,l}$	$M_j^{i,r}$
1st	1	-	19.74	-	28.24	-	29.27	-	3.65
	2	108.84	101.00	140.38	123.14	144.30	130.79	2.79	6.21
	3	55.99	60.66	94.83	97.40	91.31	92.47	-3.71	-5.06
	4	77.98	75.77	107.43	103.03	112.74	95.55	4.94	-7.26
	5	28.21	26.49	70.47	68.75	65.40	65.90	-7.19	-4.15
	6	13.94	14.88	49.81	52.36	53.92	49.44	8.25	-5.58
	7	34.75	36.63	78.37	84.53	83.46	90.80	6.49	7.42
	8	140.83	151.70	150.29	172.22	156.27	167.86	3.98	-2.53
	9	27.37	-	39.67	-	42.32	-	6.68	-

moments and inelastic moments, for the example frames, are also listed in these Tables.

The maximum % error for frame EF1 at floor level 1 is 8.26%. For frame EF2, the maximum % error at floor levels 1, 3 and 5 are 7.57%, 10.09% and 8.66% respectively. The root mean square percentage errors for frames EF1 and EF2 are 5.64% and 6.02% respectively. The root mean square

Table 7 Comparison of inelastic moments obtained from the neural networks and the hybrid procedure for frame EF2 (RH=70%)

Floor Level	Joint	Elastic moment (kN·m)		Inelastic moment (kN·m)				% error	
				Hybrid Procedure		Neural Network			
	j	$M_j^{e,l}$	$M_j^{e,r}$	$M_j^{i,l}$	$M_j^{i,r}$	$M_j^{i,l}$	$M_j^{i,r}$	$M_j^{i,l}$	$M_j^{i,r}$
1st	1	-	31.67	-	52.14	-	50.67	-	-2.81
	2	32.5	28.28	75.85	60.44	81.59	63.04	7.57	4.31
	3	26.86	29.1	63.45	66.25	67.35	65.39	6.15	-1.30
	4	41.58	56.33	67.02	92.10	63.48	95.40	-5.28	3.58
	5	45.54	-	67.35	-	71.88	-	6.72	-
3rd	1	-	27.84		53.57	-	50.98	-	-4.83
	2	24.03	23.26	74.19	69.42	81.57	67.15	9.95	-3.27
	3	32.91	33.86	73.22	74.76	80.61	73.45	10.09	-1.75
	4	42.98	52.19	80.61	95.87	77.71	88.08	-3.60	-8.12
	5	37.46	-	66.23	-	62.06	-	-6.29	-
5th	1	-	17.59		35.07	-	31.74	-	-9.49
	2	20.71	20.71	75.14	72.16	71.20	69.16	-5.24	-4.15
	3	35.69	36.12	77.04	77.57	82.46	73.93	7.05	-4.69
	4	45.73	51.1	88.88	100.09	92.26	103.19	3.80	3.10
	5	23.53	-	43.34	-	39.59	-	-8.66	-

Table 8 Ratio of sum of stiffnesses of beams to sum of stiffnesses of columns at different joints of example frames

Frame	Floor Level	Joint No. (from left to right)								
		1	2	3	4	5	6	7	8	9
EF1	1st	6.09	15.85	17.88	17.88	34.12	36.57	19.15	12.33	5.42
EF2	1st	1.03	2.40	2.40	1.71	0.69	-	-	-	-
	3rd	3.07	7.15	7.15	5.09	2.05	-	-	-	-
	5th	7.85	18.84	18.84	13.03	5.26	-	-	-	-

percentage error for both the frames is 5.87% which is acceptable for practical design. This shows the efficacy of developed neural network models for moderately high frames with any number of spans and storeys.

As has been stated earlier, ratio of beam stiffness to column stiffness has not been considered as input parameter. Table 8 shows the ratio of sum of stiffnesses of beams to sum of stiffnesses of columns meeting at each joint of floor level for which the results have been reported above. It is seen that these ratios are significantly different from each other, yet the order of error is small for practical purposes. This confirms the hypothesis made earlier that the ratio of beam stiffness to column stiffness may not be taken as input parameter.

6. Sensitivity analysis

Sensitivity studies are carried out using the developed neural networks. These studies show the influence of variations of input parameters on the output parameters.

For the sensitivity analysis, one parameter is varied while keeping the other parameters constant equal to their median values. For an internal joint, the variations of the output parameters $M_j^{e,l}/M_j^{i,l}$ and $M_j^{e,r}/M_j^{i,r}$ with the different input parameters are studied and are presented below, in turn.

R_j^l and R_j^r :- The variations of output parameters $M_j^{e,l}/M_j^{i,l}$ and $M_j^{e,r}/M_j^{i,r}$ with R_j^l and R_j^r are shown in Figs. 8 and 9 respectively. The range $R_j^l = R_j^r = 1.0-4.0$ indicates absence of cracking. In this range, the relative contribution of shrinkage, in comparison to applied loading, to $M_j^{i,l}$ and $M_j^{i,r}$, increases with increase in values of either R_j^l or R_j^r (larger values of R_j^l or R_j^r indicate smaller applied loading). Thus, decrease in $M_j^{e,l}/M_j^{i,l}$ and $M_j^{e,r}/M_j^{i,r}$ with increase in R_j^l and R_j^r is observed. It has already been stated in section 1 that the contribution of creep to $M_j^{i,l}$ and $M_j^{i,r}$ is much smaller than the contribution of shrinkage and therefore it does not affect much the variations of $M_j^{e,l}/M_j^{i,l}$ and $M_j^{e,r}/M_j^{i,r}$ with R_j^l or R_j^r.

In the ranges $R_j^l = R_j^r = 0.25-1.0$, cracking of concrete occurs in the end portions of a beam. As stated earlier in section 1, the cracking of concrete results in smaller contribution of creep and shrinkage to $M_j^{i,l}$ and $M_j^{i,r}$ as there is reduction in the portion of the concrete undergoing creep and shrinkage. There is also lowering of $M_j^{i,l}$ and $M_j^{i,r}$ resulting from instantaneous cracking as has been stated in section 1. Overall, in the range $R_j^l = R_j^r = 0.25-1.0$ also, variations are similar to the variations in the range $R_j^l = R_j^r = 1.0-4.0$.

$R_{j-1}^l, R_{j-1}^r, R_{j+1}^l$ and R_{j+1}^r :- The variations are given in Figs. 10, 11, 12 and 13 respectively. It may be noted that at the joint j itself, since R_j^l and R_j^r have been kept constant, $M_j^{e,l}$ and $M_j^{e,r}$ remain constant when $R_{j-1}^l, R_{j-1}^r, R_{j+1}^l$ and R_{j+1}^r are varied. In the range $R_{j-1}^l = R_{j-1}^r = R_{j+1}^l = R_{j+1}^r = 1.0-4.0$, cracking at joints $j-1$ and $j+1$ is absent, contribution of shrinkage to $M_j^{i,l}$ and $M_j^{i,r}$ therefore does not change with changes in values of these parameters. Further, since the effect of creep is also small, $M_j^{i,l}$ and $M_j^{i,r}$ do not change much in this range. Therefore, only small variations of $M_j^{e,l}/M_j^{i,l}$ and $M_j^{e,r}/M_j^{i,r}$ are observed in the range $R_{j-1}^l = R_{j-1}^r = R_{j+1}^l = R_{j+1}^r = 1.0-4.0$.

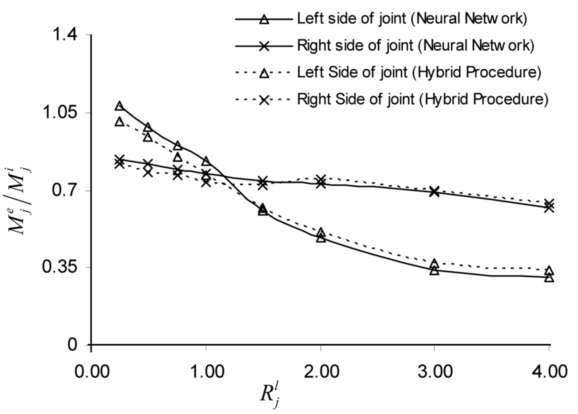

Fig. 8 Variation of $M_j^{e,l}/M_j^{i,l}$ and $M_j^{e,r}/M_j^{i,r}$ with R_j^l for an internal joint

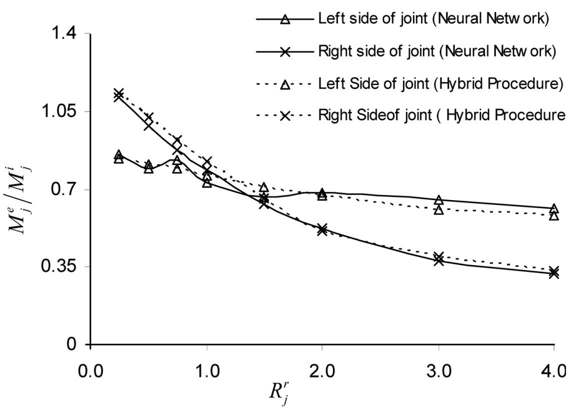

Fig. 9 Variation of $M_j^{e,l}/M_j^{i,l}$ and $M_j^{e,r}/M_j^{i,r}$ with R_j^r for an internal joint

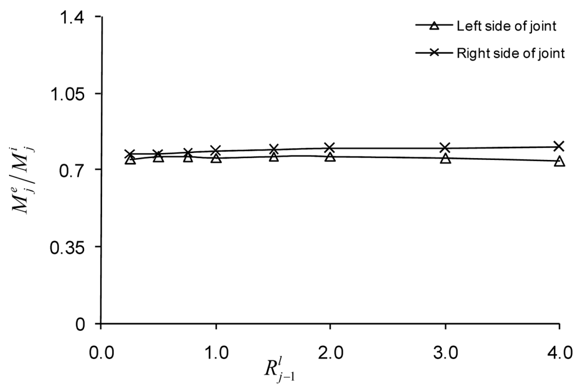

Fig. 10 Variation of $M_j^{e,l}/M_j^{i,l}$ and $M_j^{e,r}/M_j^{i,r}$ with R_{j-1}^l for an internal joint

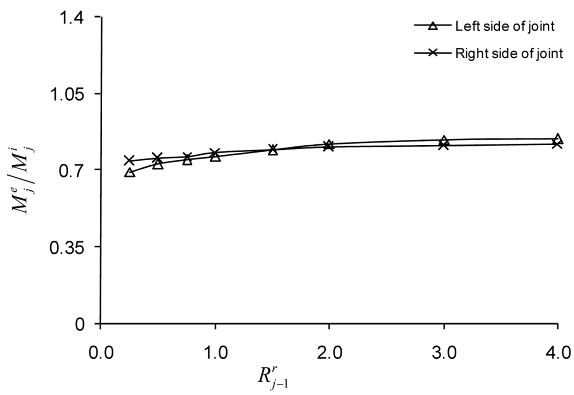

Fig. 11 Variation of $M_j^{e,l}/M_j^{i,l}$ and $M_j^{e,r}/M_j^{i,r}$ with R_{j-1}^r for an internal joint

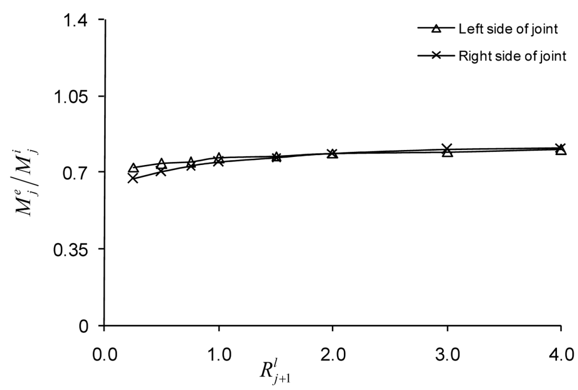

Fig. 12 Variation of $M_j^{e,l}/M_j^{i,l}$ and $M_j^{e,r}/M_j^{i,r}$ with R_{j+1}^l for an internal joint

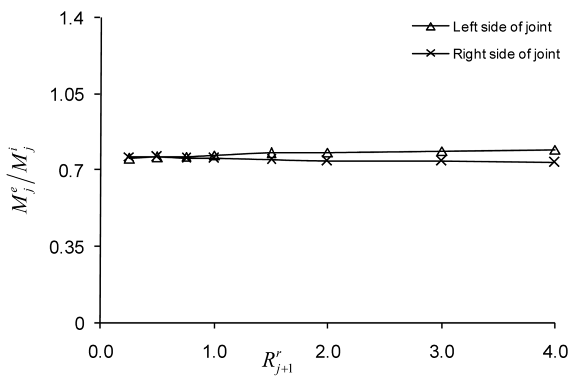

Fig. 13 Variation of $M_j^{e,l}/M_j^{i,l}$ and $M_j^{e,r}/M_j^{i,r}$ with R_{j+1}^r for an internal joint

In the range $R_{j-1}^l = R_{j-1}^r = R_{j+1}^l = R_{j+1}^r = 0.25 - 1.0$, cracking occurs at joints $j-1$ and $j+1$. As indicated in section 1, cracking at these joints results in higher moments $M_j^{i,l}$ and $M_j^{i,r}$ at the adjacent joint j. Since cracking reduces with increasing values of $R_{j-1}^l, R_{j-1}^r, R_{j+1}^l$ and R_{j+1}^r, in the range 0.25-1.0, $M_j^{i,l}$ and $M_j^{i,r}$ become smaller with increasing values of $R_{j-1}^l, R_{j-1}^r, R_{j+1}^l$ and R_{j+1}^r in this range. This results in variations shown in Figs. 10-13.

It is observed that the influence of a cracking moment ratio, $R_{j-1}^l, R_{j-1}^r, R_j^l, R_j^r, R_{j+1}^l$ and R_{j+1}^r on left side or right side of a joint $k(=j-1, j, j+1)$, on the output parameters, $M_j^{e,l}/M_j^{i,l}$ and $M_j^{e,r}/M_j^{i,r}$, at a side of the joint j, reduces as the position of the side at the joint k increases from the side at joint j. Similar observation has been made earlier (Pendharkar 2007).

S_{j-1}/S_j and w_{j-1}/w_j :- The variations are shown in Figs. 14 and 15 respectively. The cracking moment ratios R_{j-1}^l, R_{j-1}^r, R_j^l, R_j^r, R_{j+1}^l and R_{j+1}^r are kept constant as S_{j-1}/S_j and w_{j-1}/w_j are varied. Thus, with the elastic moments at the joints remaining constant, differing elastic moment distributions in spans $j-1$ and j resulting from different values of S_{j-1}/S_j and w_{j-1}/w_j would not contribute significantly to $M_j^{i,l}$ and $M_j^{i,r}$. Therefore, not much variation is observed for $M_j^{e,l}/M_j^{i,l}$ and $M_j^{e,r}/M_j^{i,r}$.

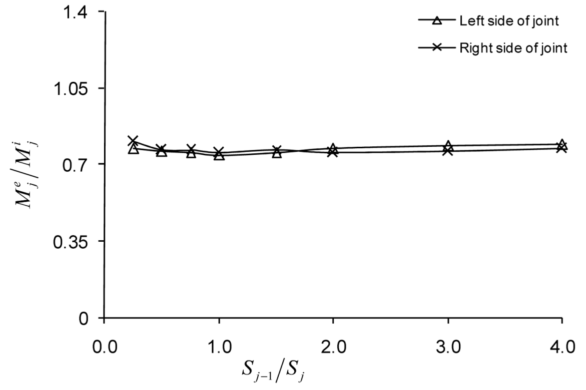

Fig. 14 Variation of $M_j^{e,l}/M_j^{i,l}$ and $M_j^{e,r}/M_j^{i,r}$ with S_{j-1}/S_j for an internal joint

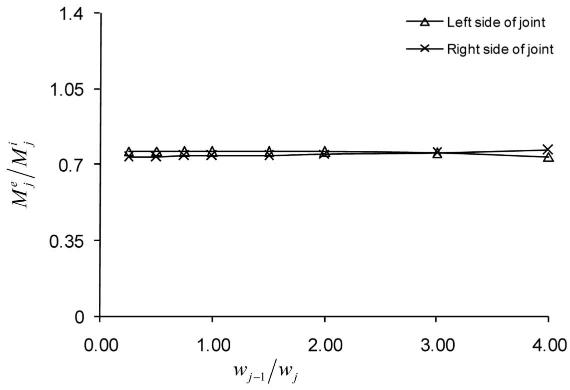

Fig. 15 Variation of $M_j^{e,l}/M_j^{i,l}$ and $M_j^{e,r}/M_j^{i,r}$ with w_{j-1}/w_j for an internal joint

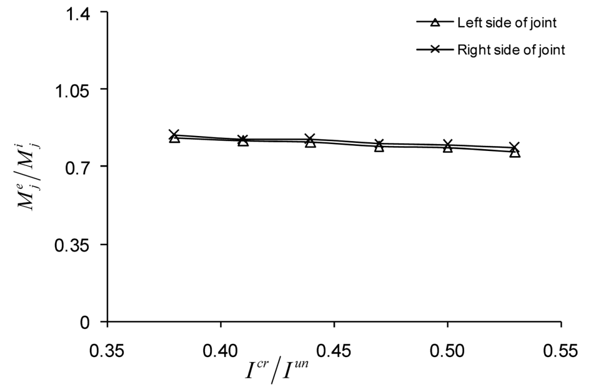

Fig. 16 Variation of $M_j^{e,l}/M_j^{i,l}$ and $M_j^{e,r}/M_j^{i,r}$ with I^{cr}/I^{un} for an internal joint

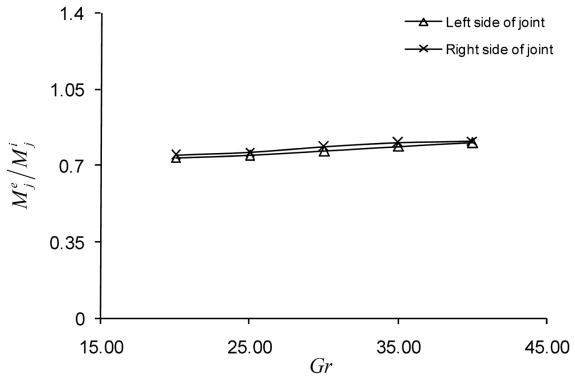

Fig. 17 Variation of $M_j^{e,l}/M_j^{i,l}$ and $M_j^{e,r}/M_j^{i,r}$ with *Gr* for an internal joint

I^{cr}/I^{un}:- The variations are shown in Fig. 16. Increasing values of I^{cr}/I^{un} result in smaller effect of instantaneous cracking and therefore in higher values of $M_j^{i,l}$ and $M_j^{i,r}$. Further, smaller cracking would also result in greater shrinkage and creep effects, as stated in section 1, and therefore in higher values of $M_j^{i,l}$ and $M_j^{i,r}$. This results in reduction in $M_j^{e,l}/M_j^{i,l}$ and $M_j^{e,r}/M_j^{i,r}$ with increasing I^{cr}/I^{un}.

Gr:- The variations are shown in Fig. 17. With increasing *Gr*, tensile strength of concrete increases, instantaneous cracking of concrete decreases and, therefore, $M_j^{i,l}$ and $M_j^{i,r}$ increase. As stated in the previous paragraph, smaller concrete cracking also results in higher values of $M_j^{i,l}$ and $M_j^{i,r}$ on account of creep and shrinkage. On the other hand, the creep coefficient and shrinkage strain would reduce with increase in *Gr* (CEB-FIP MC 90 1993). This would result in lesser value of $M_j^{i,l}$ and $M_j^{i,r}$. The net result is therefore gradual increase in $M_j^{e,l}/M_j^{i,l}$ and $M_j^{e,r}/M_j^{i,r}$ with increasing *Gr*.

t_0:- The variations are shown in Fig. 18. The tensile strength of concrete increases and creep coefficient decreases with increase in age of loading (CEB-FIP MC 90 1993). The variations of $M_j^{e,l}/M_j^{i,l}$ and $M_j^{e,r}/M_j^{i,r}$ with t_0 are therefore similar to those of $M_j^{e,l}/M_j^{i,l}$ and $M_j^{e,r}/M_j^{i,r}$ with *Gr*.

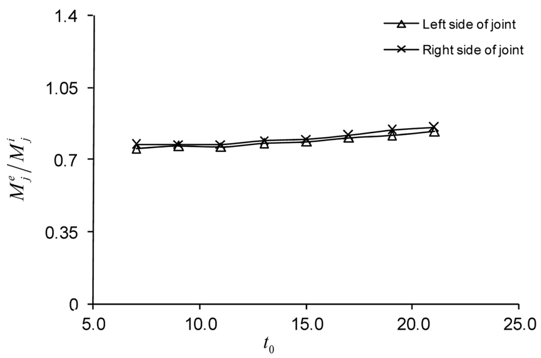

Fig. 18 Variation of $M_j^{e,l}/M_j^{i,l}$ and $M_j^{e,r}/M_j^{i,r}$ with t_0 for an internal joint

7. Results and discussion

The percentage change in the output parameters, within the range of each input parameter, is summarized in Table 9. It is observed that out of the eleven input parameters considered, the most sensitive parameters affecting the output parameters are R_j^l and R_j^r for $M_j^{e,l}/M_j^{i,l}$ and $M_j^{e,r}/M_j^{i,r}$ respectively. The next most sensitive parameters are R_{j-1}^l and R_{j+1}^l. Further, it is observed that the influence of parameters R_{j-1}^l and R_{j-1}^r is small. The effect of S_{j-1}/S_j, w_{j-1}/w_j, I^{cr}/I^{un}, Gr and t_0 is also found to be small in the sensitivity analysis.

It is of interest to compare these observations, for composite frames, with the observations of the earlier studies carried out by Chaudhary *et al.* (2007c) and Pendharkar *et al.* (2007) for the continuous composite beams. As stated earlier in section 1, Chaudhary *et al.* (2007c) considered the cracking effect only whereas Pendharkar *et al.* (2007) considered both cracking and time-dependent effects. Cracking moment ratio at the support (pertaining to the output parameter) has been found to be the most significant input parameter earlier also by Pendharkar *et al.* (2007) for the continuous composite beams. Further, similar observations of reduction of influence of cracking moment ratio at a support with increase in the distance from the support (pertaining to the output parameter) has been made by Pendharkar *et al.* (2007) and Chaudhary *et al.* (2007c) for continuous composite beams. The smaller effect S_{j-1}/S_j, w_{j-1}/w_j, I^{cr}/I^{un}, Gr and t_0 has been observed earlier also by Pendharkar *et al.* (2007).

The values of output parameters obtained from the hybrid procedure and neural networks are also compared for the most significant input parameters, R_j^l and R_j^r and are found to be quite close (Figs. 8 and 9).

Table 9 Percentage change in output parameter within range of each input parameter

Output Parameter	Percentage Change										
	Input Parameters										
	$\frac{S_{j-1}}{S_j}$	$\frac{w_{j-1}}{w_j}$	R_{j-1}^l	R_{j-1}^r	R_j^l	R_j^r	R_{j+1}^l	R_{j+1}^r	$\frac{I^{cr}}{I^{un}}$	Gr (N/mm^2)	t_0 (days)
$M_j^{e,l}/M_j^{i,l}$	6.94	4.11	2.74	21.74	251.61	40.98	11.11	5.33	7.79	9.59	10.67
$M_j^{e,r}/M_j^{i,r}$	9.59	4.11	3.90	10.21	35.48	246.88	22.73	4.11	7.69	9.46	10.39

8. Conclusions

A methodology has been presented for predicting inelastic bending moments in large composite frames from elastic bending moments by using neural network models. The methodology has been demonstrated for moderately high composite frames by developing two neural network models. The two models, Net-external and Net-internal, are applicable for external and internal joints respectively. The models have been validated with the example frames and sensitivity analysis is also carried out to identify the important parameters affecting the output parameters. The following are the important findings of the study.

1. The most significant parameters affecting the values $M_j^{e,l}/M_j^{i,l}$ and $M_j^{e,r}/M_j^{i,r}$ are R_j^l and R_j^r are respectively.
2. The developed neural network models can predict inelastic moments with reasonable accuracy from the elastic moments, which in turn, can be obtained from any of the readily available software.
3. The overall root mean square percentage error for the example frames, considered for validation is about 6%, which is acceptable for practical design.
4. The neural networks are applicable for moderately high composite frames of any number of spans and storeys.

The methodology can be used for developing the neural networks for rapid prediction of inelastic bending moments for high rise composite frames also.

Acknowledgements

The authors gratefully acknowledge the support given by DST, Govt. of India under grant no. R/S3/MERC/0023/2008.

References

Akbas, B. (2006), "A neural network model to assess the hysteretic energy demand in steel moment resisting frames", *Struct. Eng. Mech.*, **23**(2), 177-193.

Amadio, C. and Fragiacomo, M. (1997), "A simplified approach to evaluate creep and shrinkage effects in steel concrete composite beams", *J. Struct. Eng.-ASCE*, **123**(9), 1153-1162.

Arslan, M.H., Ceylan, M., Kaltakci, M.Y., Ozaby, Y. and Gulay, F.G. (2007), "Prediction of force reduction factor (R) of prefabricated industrial buildings using neural networks", *Struct. Eng. Mech.*, **27**(2), 117-134.

Bakhary, N., Hao, H. and Deeks, A.J. (2007), "Damage detection using artificial neural network with consideration of uncertainties", *Eng. Struct.*, **29**(11), 2806-2815.

Bazant, Z.P. (1972), "Prediction of concrete creep-effects using age adjusted effective modulus method", *ACI J.*, **69**(4), 212-217.

Bradford, M.A., Manh, H.V. and Gilbert, R.I. (2002), "Numerical analysis of continuous composite beams at service loading", *Adv. Struct. Eng.*, **5**(1), 1-12.

CEB-FIP MC 90 (1993), Model Code 1990 for Concrete Structures. Bulletin d' information No. 213/214. *Comite´ Euro International du Beton-Fe´de´ration International de la Pre´contrainte*, Laussane, Switzerland.

Chandak, R., Upadhyay, A. and Bhargava, P. (2008), "Shear lag prediction in symmetrical laminated composite box beams using artificial network", *Struct. Eng. Mech.*, **29**(1), 77-89.

Chang, S., Kim, D., Chang, C. and Cho, S.G. (2009), "Active response control of an offshore structure under wave loads using the modified probabilistic neural network", *J. Mater. Sci. Technol.,* **14**(2), 240.

Chaudhary, S., Pendharkar, U. and Nagpal, A.K. (2007a), "Service load behavior of low rise composite frames considering creep, shrinkage and cracking", *Latin Am. J. Solids Struct.*, **5**(4), 237-258.

Chaudhary, S., Pendharkar, U. and Nagpal, A.K. (2007b), "A hybrid procedure for cracking and time-dependent effects in composite frames at service load", *J. Struct. Eng.-ASCE*, **133**(2), 166-175.

Chaudhary, S., Pendharkar, U. and Nagpal, A.K. (2007c), "Bending moment prediction for continuous composite beams by neural networks", *Adv. Struct. Eng.*, **10**(4), 439-454.

Cheng, J., Cai, C.S. and Xiao, R.C. (2007), "Application of artificial neural networks to the response prediction of geometrically nonlinear truss structures", *Struct. Eng. Mech.,* **26**(3), 251-262.

Cho, H.N., Cho, Y.M., Lee, S.C. and Hur, C.K. (2004), "Damage assessment of cable stayed bridges using probabilistic neural network", *Struct. Eng. Mech.*, **17**(3), 483-492.

Cruz, P.J.S., Mari, A.R. and Roca, P. (1998), "Non-linear time dependent analysis of segmentally constructed structures", *J. Struct. Eng.-ASCE*, **124**(3), 278-287.

Fragiacomo, M., Amadio, C. and Macorini, L. (2004), "Finite element model for collapse and long-term analysis of steel-concrete composite beams", *J. Struct. Eng.-ASCE*, **130**(3), 489-497.

Ghali, A., Favre, R. and Elbadry, M. (2002), *Concrete Structures: Stresses and Deformations*, Third Edition, Spon Press, London.

Gilbert, R.I. and Bradford, M.A. (1995), "Time-dependent behavior of composite beams at service loads", *J. Struct. Eng.-ASCE*, **121**(2), 319-327.

Giri, V. and Upadhyay, A. (2006), "ANN based prediction of moment coefficients in slabs subjected to patch load", *Struct. Eng. Mech.*, **24**(4), 509-514.

Jeng, C.H. and Mo, Y.L. (2004), "Quick seismic response estimation of prestressed concrete bridges using artificial neural networks", *J. Comput. Civil Eng.-ASCE*, **118**(4), 360-369.

Jiang, S.F., Zhang, C.M. and Koh, C.G. (2006), "Structural damage detection by integrating data fusion and probabilistic neural network", *Adv. Struct. Eng.*, **9**(4), 445-458.

Kim, D.H., Kim, D. and Chang, S.K. (2009a), "Application of lattice probabilistic neural network for active response control of offshore structures", *Struct. Eng. Mech.,* **31**(2), 153-162.

Kim, D., Kim, D.H., Cui, J., Seo, H.Y. and Lee, Y.H. (2009b), "Iterative neural network strategy for static model identification of an FRP deck", *Steel Compos. Struct.,* **9**(5), 445-455.

Kwak, H.G. and Seo, Y.J. (2000), "Long term behavior of composite girder bridges", *Comput. Struct.*, **74**(5), 583-599.

Lee, J.J., Lee, J.W., Yi, J.H., Yun, C.B. and Jung, H.Y. (2005), "Neural network-based damage detection for bridges considering errors in baseline finite element models", *J. Sound Vib.*, **280**(3-5), 555-578.

Mari, A. (2000), "Numerical simulation of the segmental construction of three dimensional concrete frames", *Eng. Struct.*, **22**(6), 585-596.

Mo, Y.L., Hung, H.Y. and Zhong, J. (2002), "Investigation of stress-strain relationship of confined concrete in hollow bridge columns using neural networks", *Journal of Testing and Evaluation*, ASTM, **30**(4), 330-339.

Pendharkar, U. (2007), "Neural network model for composite beams and frames considering cracking and time-effects", Ph.D. Thesis, IIT Delhi, Delhi.

Pendharkar, U., Chaudhary, S. and Nagpal, A.K. (2007), "Neural network for bending moment in continuous composite beams considering cracking and time effects in concrete", *Eng. Struct.*, **29**(9), 2069-2079.

Pendharkar, U., Chaudhary, S. and Nagpal, A.K. (2010), "Neural networks for inelastic mid-span deflections in continuous composite beams", *Struct. Eng. Mech.*, **36**(2), 165-179.

SNNS (1998), User's Manual, Ver. 4.2*, University of Sttutgart, Institute for Parallel and Distributed High Performance Systems.*

Yeung, W.T. and Smith, J.W. (2005), "Damage detection in bridges using neural networks for pattern recognition of vibration signatures", *Eng. Struct.*, **27**(5), 685-698.

Notations

E	: modulus of elasticity of concrete
Gr	: grade of concrete
I^{un}	: transformed moment of inertia of composite section
I^{cr}	: moment of inertia of steel section
M^{cr}, M^{e}, M^{i}	: bending moments
R^{l}_{j-1}, R^{r}_{j-1}, R^{l}_{j}, R^{r}_{j}, R^{l}_{j+1}, R^{r}_{j+1}	: cracking moment ratios
RH, RH_1, RH_2	: relative humidities
S_{j-1}, S_j	: stiffnesses
S_{j-1}/S_j	: stiffness ratios
l	: span length
n	: number of spans/bays
t_0	: age of loading
w	: uniformly distributed load

Subscript

e	: age-adjusted properties
j	: support or span number

Superscript

cr	: cracking
e	: elastic
i	: inelastic
l	: left side of a joint
r	: right side of a joint